FAM83A is a Potential Biomarker for Breast Cancer Initiation

Natascia Marino (marinon@iu.edu)
Indiana University https://orcid.org/0000-0001-6771-8963
Rana German
IU Simon Cancer Center: Indiana University Melvin and Bren Simon Cancer Center
Ram Podicheti
Indiana University Bloomington
Pam Rockey
IU Simon Cancer Center: Indiana University Melvin and Bren Simon Cancer Center
George E. Sandusky
Indiana University School of Medicine
Constance J. Temm
Indiana University School of Medicine
Harikrishna Nakshatri
Indiana University School of Medicine
Rebekah J. Addison
Indiana University School of Medicine
Bryce Selman
Indiana University School of Medicine
Sandra K. Althouse
Indiana University School of Medicine
Anna Maria V. Storniolo
Indiana University School of Medicine

Research

Keywords: normal breast, FAM83A, breast cancer, cell transformation

Posted Date: October 26th, 2021

DOI: https://doi.org/10.21203/rs.3.rs-995694/v1

Version of Record: A version of this preprint was published at Biomarker Research on February 19th, 2022. See the published version at https://doi.org/10.1186/s40364-022-00353-9.

Abstract

Background: Family with sequence similarity 83 member A (FAM83A) presents oncogenic properties in several cancers including breast cancer (BC). Recently, we reported FAM83A overexpression in normal breast tissues from women at high risk of breast cancer. We now hypothesize that FAM83A is a key factor in BC initiation.

Methods: Immunohistochemical staining was used to evaluate FAM83A protein levels in both a normal breast tissue microarray (TMA, N=411) and a breast tumor TMA (N=349). EGFR staining and its correlation with FAM83A expression were also assessed. Lentivirus-mediated manipulation of FAM83A expression in primary and hTERT-immortalized breast epithelial cells was employed. Biological and molecular alterations upon FAM83A overexpression/downregulation and FAM83A's interaction partners were investigated.

Results: TMA analysis revealed a 1.5-fold increase in FAM83A expression level in BC cases as compared with normal breast tissues (p<0.0001). FAM83A protein expression was directly correlated with EGFR level in both normal and BC tissues. In *in vitro* assays, exogenous expression of FAM83A in either primary or immortalized breast epithelial cells promoted cell viability and proliferation. Additionally, Ingenuity Pathway Analysis (IPA) revealed that in normal cells FAM83A is involved in cellular morphology and metabolism. Mass spectrometry analysis identified DDX3X and LAMB3 as potential FAM83A interaction partners in primary cells, while we detected FAM83A interaction with cytoskeleton reorganization factors, including LIMA1, MYH10, PLEC, MYL6 in the immortalized cells.

Conclusions: This study shows that FAM83A promotes metabolic activation in primary epithelial cells and survival in immortalized cells. These findings support its role in early breast oncogenesis.

Background

Though significant strides have been made in the last several decades in both early diagnosis and treatment of breast cancer, our ability to prevent the disease remains limited by our lack of understanding of the earliest changes of cancer initiation.

Because of their involvement in cancer cell signaling and overexpression in several cancers, the FAM83 proteins are emerging as potential oncogenes (1). FAM83 (family with sequence similarity 83) consists of 8 genes, named FAM83A-H, each located at a distinct genomic site and characterized by a highly conserved domain of unknown function, the DUF1669 domain, in the N-terminus (2, 3). FAM83 gene expression is reported increased relative to relevant normal tissues in a number of cancers, including breast, lung, ovary, cervical, testis, thyroid, bladder, and lymphoid cancers (3, 4).

We recently reported the upregulation of FAM83A in cancer-free breast tissues from women at high risk of developing breast cancer compared with breasts from average-risk women (5). FAM83A, a 434-amino acid protein, shares the DUF1669 with other FAM83 members and contains serine-rich and proline-rich

domains (6-8). FAM83A has been reported to regulate the EGFR pathway in breast cancer cells, leading to the development of resistance to tyrosine kinase inhibitors (TKIs) (4, 6, 9). Furthermore, FAM83A accelerated cell migration and invasion through the activation of epithelial-mesenchymal transition (EMT) via PI3K/ATK/Snail signaling (2, 8, 10). Additionally, FAM83A upregulation was identified in multiple human tumor types, including breast (6, 8, 9), pancreatic (11) and ovarian (1) cancers, as well as lung adenocarcinoma (12). A meta-analysis reported that patients with breast cancer with high expression of FAM83A exhibited elevated tumor grade and a poor clinical prognosis (13). Based on the aforementioned studies, FAM83A is considered to be a candidate oncogene. Nevertheless, the role of FAM83A in the development and progression of breast cancer is not fully understood. Among the identified molecular mechanisms, FAM83A is involved in the regulation of the ErbB signaling network, both at the receptor level and the downstream MAPK pathway (2).

The present study examined the role of FAM83A in the normal breast and in the early phases of BC development. First, FAM83A overexpression in BC and its correlation with EGFR was evaluated using a large cohort of either normal or cancerous breast tissues. FAM83A overexpression in both primary and immortalized breast epithelial cells promoted metabolic activation and cell proliferation. Finally, we identified differences in FAM83A's interaction partners between primary and immortalized cells. These findings support the role of FAM83A in breast cancer initiation and, thus, as a potential biomarker for breast cancer susceptibility.

Methods

Tissue Microarray (TMA) and Immunohistochemistry

Normal breast and breast cancer (BC) TMAs were obtained from the Susan G. Komen Tissue Bank at IU Simon Comprehensive Cancer Center (KTB) under Institutional Review Board (IRB) protocol #1011003097 and IUSCCC Tissue Procurement and Distribution Core under IRB protocol #**11438**, respectively. Demographics and staining data are reported in **Additional File 1: Table S1** and **S2**. The TMAs were stained with antibodies specific for FAM83A (Protein Tech 20618-1-AP, 1:100) and EGFR (Agilent, K149489, 1:400). Each different antibody underwent a "workup" to determine which steps (or protocol) would best demonstrate the antibody on a particular tissue slide. After de-paraffinizing, TMA sections (4μm for tumor TMAs and 6μm for the normal breast TMA) mounted on DAKO slides were subjected to high pH antigen retrieval in the Dako Link PT module. The antibody testing was run on a Dako Link48 with primary antibody for 20 min, Flex-HRP 20 min followed by detection with DAB for 10 min. Three pathologists utilized light microscopy (Leica) to evaluate the staining in each tissue core (range from negative, slight, moderate, or severe) on the immunostainings. The slides were imaged using the Aperio Scanscope CS. Computer-assistedmorphometric analysis of digital images was performed using the Aperio Image Analysis software that came with the Aperio Whole Slide Digital Imaging System (14). The Positive Pixel Count algorithm was used to quantify the amount of a specific stain present in a scanned slide image. The H score was calculated using the Aperio TMA software algorithm (14).

Cell culture and *in vitro* assays

Primary breast epithelial cells were isolated and cultures as previously described (15). H-TERT immortalization was obtained upon lentiviral infection of the primary cells with hTERT-expressing lentivirus (Cat# LVP1130 Amsbio, Cambridge MA). H-TERT immortalized cells were then cultured as previously described (16). Lentiviral infection: Lentivirus containing plasmids encoding shRNAs targeting FAM83A or GFP in pLKO.1 were acquired from Sigma-Aldrich (Sigma Aldrich; sh83A2 TRCN0000168628, sh83A6 TRCN000168368) [33]. GFP-FAM83A or GFP expressing lentivirus particles were obtained from Origene (Lenti ORF particles, FAM83A (mGFP-tagged, transcript 1(CAT#: RC208565L4V) and transcript 2 (Cat# RC219879L4V); Lenti ORF control particles of pLenti-C-mGFP-P2A-Puro, CAT#: PS100093V). Lentivirus at MOI 20 was supplemented with 8 µg/ml polybrene (Santa Cruz) and ViralPlus Transduction Enhancer (Abm, Richmond, BC, Canada, cat: G698, dilution 1:100) before being added to the cell culture. Cells were infected with virus for 16 hours. Cell proliferation was evaluated by using the following assays: BrdU Proliferation Assay: The BrdU cell proliferation assay was conducted according to the manufacturer's protocol (MilliporeSigma, Burlington, MA). The cells were cultured in 96-well plates at a density of $1x10^4$ cells/well for 72 hr. Twenty-four hours prior, the cells were labeled with BrdU and tagged with the anti-BrdU antibody. Afterwards the substrate was added to the wells, and the colored product was measured using the plate reader (Bio-tek Instruments, USA) at 450 nm. *Sulforhodamine B (*SRB) assay: The SRB assay is used for cell density determination, based on the measurement of cellular protein content. $1x10^4$ cells/well were cultured in 96-well plates for either 24h or 96h. After an incubation period, cell monolayers were fixed with 10% (wt/vol) trichloroacetic acid and stained for 30 min; then, excess dye was removed by washing the cells repeatedly with 1% (vol/vol) acetic acid. The protein-bound dye was dissolved in 10 mM Tris base solution for optical density, or absorbance, determination at 510 nm using a microplate reader. Experiments included at least four technical duplicates for each condition and were performed three times. The data are shown as percentage of cell-growth calculated using the following equations: %Cell growth=(MeanODsample/MeanODctr)×100.

RNA isolation and real-time quantitative PCR (qPCR)

Total RNA was extracted from cells using AllPrep DNA/RNA/miRNA kit (Qiagen). Reverse transcription was performed using SuperScript™ IV VILO™ Master Mix (Invitrogen cat#: 11756050) according to the manufacturer's instructions. qPCR was performed using the TaqMan™ Universal PCR Master Mix (Applied Biosystems, cat# 4304437) and the following TaqMan Gene Expression Assays (Applied Biosystems/Thermo Fisher Scientific, Grand Island, NY):ACTB (Hs99999903_m1), FAM83A (Hs04994801_m1), and NEK2 (Hs00601227_m1).qPCR reactions were run on a StepOne Plus Real-Time PCR System (Applied Biosystems/Thermo Fisher Scientific) and data analyzed using the StepOne Software v2.3 (Applied Biosystems). Relative quantification was calculated with reference to ACTB and analyzed using the comparative C_T method. qPCR experiments were performed in triplicate.

Mass Spectrometry

Cells were lysed in NP40 lysis buffer (150mM NaCl, 1% NP-40, 50mM Tris-Cl pH 8.0) plus Protease Inhibitor Cocktail (Sigma P8340) plus PhosSTOP (Sigma 4906845001). Cell extracts containing equal quantities of proteins, determined using the BCA Protein Assay kit (Pierce-Thermo Scientific, #23227), were incubated overnight at 4 °C with anti-GFP beads (mGFP/mCFP/mYFP/KillerRed Monoclonal Antibody (OTI2F6), Magnetic beads, TrueMAB, Origene). After 3x washes with PBS, the samples were then submitted to the IUSM Proteomic Core. The resin and bound proteins were removed from the lysate by gravity flow through a 30mL Bio-Rad Econoprep column and washed on the column with 60 mL TAP lysis buffer. The resin was resuspended 300µL of 50mM Ammonium bicarbonate pH 8.0 and transfer to a microcentrifuge tube for on bead digestion with 5µL of Trypsin Gold (0.1µg/µL) overnight with shaking at 37°C. The supernatant containing the digested proteins was removed and treated with 20µL of 90% formic acid to inactivate the trypsin. Samples were processed with onbead digestion protocol, cleaned up on spin columns, and ¼ of each was injected on the Eclipse Orbitrap mass spectrometer Thermo Fisher) with FAIMS pro interface (17). The raw files were searched against the reviewed human UNIPROT database and common contaminants and loaded into Scaffold for easy comparison and viewing.

Transcriptome analysis

Normal breast tissues from either women prior to their BC diagnosis (susceptible normal, (15)) or age-matched healthy women were obtained from the Susan G. Komen Tissue Bank at IUSCCC (**Additional File 1: Table S3**). Subjects were recruited under a protocol approved by the Indiana University Institutional Review Board (IRB protocol number 1011003097 and 1607623663). Total RNA was extracted from fresh frozen breast tissues using 3mm zirconium beads (Benchmark Scientific, cat.# D1032-30) and the AllPrep DNA/RNA/miRNA kit (Qiagen) as previously described (5). Then, cDNA library was prepared using the TruSeq Stranded Total RNA Kit (Illumina, San Diego, CA) and sequenced using Illumina HiSeq4000. Cleaned reads mapped to Human genome reference sequence GRCh38.p12 with gencode v.28 annotation, using STAR version STAR_2.5.2b (18). Differential Expression Analysis was performed using DESeq2 ver. 1.12.3. The *p*values from the *t*-test were corrected for multiple testing using Benjamini-Hochberg method.

The dataset is available in the Gene Expression Omnibus (GEO) repository (accession number GSE166044, https://www.ncbi.nlm.nih.gov/geo/query/acc.cgi?acc=GSE166044). Transcriptome profiling of primary breast epithelial cells (N=3) overexpressing either the empty vector (mock, CTR) or FAM83A was performed using Clontech SMARTer Stranded Total RNA-Seq Kit v2 for generating the library, followed by sequencing on NovaSeq v1.5 S4 (200 cycles).

Data analysis

Ingenuity Pathways Analysis (IPA, Qiagen, Redwood City, CA) was used for canonical pathway, upstream regulator and gene network analyses (19). Publicly available transcriptomic data of microdissected-breast epithelial samples from either susceptible or matched healthy were obtained from GEO with accession number GSE141828 (https://www.ncbi.nlm.nih.gov/geo/query/acc.cgi?acc=GSE141828), respectively. Genomic alterations and expression analyses of *The Cancer Genome Atlas (TCGA, N=3255*

for genomic alteration and N=983 for mRNA) and the Molecular Taxonomy of Breast Cancer International Consortium (METABRIC, N=1904 for genetic alteration and N=1405 for mRNA) (20, 21) were performed by interrogating cBioPortal (https://www.cbioportal.org/) database (22).

Statistical analysis.

Comparisons between groups were done using either Student's *t*-test or nonparametric Mann-Whitney test on GraphPad Prism 9. Difference between groups is considered significant at *p*-values<0.05. For the tissue microarray (TMA) data analysis was conducted using SAS software version 9.4 (SAS Institute Inc., Cary, NC). Baseline demographic characteristics were summarized as median (range) for continuous variables and number and percentage for categorical variables. Comparisons between groups for H-Score and Positivity used a t-test to compare results to normal tissue. Correlations were also tested for the patients with both EGFR and FAM83A observations for positivity and H-score using the Wilcoxon test and Pearson's correlation co-efficient. Finally, FAM83A H-scores and Positivity were divided into low and high categories at the score of 29.84702 (h-score) and 0.168319 (positivity) for overall survival (time from surgery to death or censoring). These cutoff values were determined by using the maximum chi-square value for all score values between the 25th and 75th percentile (http://www.pharmasug.org/proceedings/2012/SP/PharmaSUG-2012-SP12.pdf). Kaplan-Meier analysis was used to analyze the data and used the log-rank p-value to compare the two groups.

Results

FAM83A protein upregulation in breast cancer

FAM83A was first discovered for its ability to induce cell transformation in breast epithelial cells (6). The *FAM83A* locus is located on chromosome 8q24.13, which is frequently amplified in a number of human cancers (23). Analysis of FAM83A genomic aberrations in either the METABRIC or TCGA dataset revealed FAM83A locus amplification in 23% or 15% of BC, respectively (**Additional File 2: Supplementary Fig. 1A**). Overexpression of FAM83A protein level in Her2 positive (HER2+) BC was previously reported (8), and FAM83A mRNA upregulation in HER2+ BC was also detected in TCGA and METABRIC databases (**Additional File 2**: **Supplementary Fig. 1B-C**).

Here, we examined the expression of FAM83A in both normal breast tissues (N=411) and breast cancer (BC) cases (N=349) (**Figure 1A** and **B, Additional File 1: Table S1 and S2**). Immunohistochemical analysis revealed a 1.5-fold increase in FAM83A protein levels in breast tumors as compared with the normal breasts (*p*=5E-13). In our TMA analysis we observed an increase in FAM83A protein in estrogen and progesterone receptor (ER and PR) positive BC as well as in HER2+ BC as compared with normal breasts (**Figure 1C**, *p*=3E-11, *p*=1E-08 and *p*=0.002, respectively for Positivity analysis, and *p*=1E-11, *p*=1E-08, and *p*=0.002, respectively, for H-score analysis). FAM83A was overexpressed in early stages of BC (T1, *p*=1.8E-12 and T2, *p*=6E-07 for both Positivity and H-score analyses) more than in the later stages (T3, *p*=0.001 and T4, *p*=0.01 for Positivity; T3, *p*=0.001 and T4, *p*=0.008 for H-score, **Figure 1D**). No differences in FAM83A levels in relation with lymph node positivity (N) and metastatic disease (M) were

observed (**Additional File 2**: **Supplementary Fig 1D** and **E**). Moreover, Kaplan-Meier curves indicated that the overall survival was significantly poor in high FAM83A expression BC cases as compared with the cases with low FAM83A expression (p=0.02 for positivity data; p=0.04 for H-score data; **Figure 1E**).

FAM83A expression increased in early phase of BC development

We recently reported FAM83A upregulation in normal breasts from women at high risk of developing breast cancer as compared with breasts from average-risk women, according to the Tyrer-Cuzick risk estimation model (5). The correlation of FAM83A protein level with the estimated risk score was confirmed by using an independent immunostaining of our large sample cohort (**Additional File 2**: **Supplementary Fig. 2A**). Then, we examined FAM83A expression in histologically normal breast tissues from either healthy women (healthy control, HC) or women who had later a diagnosis of breast cancer (susceptible normal, Susc) retrieved from the GSE141828 dataset (**Figure 2**) (15). Only data points with >10 reads were included into the analysis. FAM83A showed a 3.9-fold increased expression in Susc (N=4) as compared with the HC (N=8) (p=0.02) (**Figure 2A**). To confirm these data, we performed a transcriptomic analysis of whole breast tissue from an independent cohort of either HC or Susc (**Additional File 1**: **Table S3)**. FAM83A expression showed a 1.9-fold increase in Susc (N=3) breasts as compared with HC samples (N=8) (p=0.03; **Figure 2B**), suggesting an upregulation of FAM83A in early phase of breast cancer development. To verify our observation, we analyzed the dataset generated by Aran *et al* (24) including transcriptome profiling of normal breast (from the GTEx database), normal adjacent to tumor (NAT, from the TCGA database) and breast tumors (from TCGA). FAM83A expression increased in the (NAT) compared with the normal breast (logFoldChange: 3.96, p=9.9E-20, and also compared with the tumor (logFoldChange: 2.69, p=1.0E-18) (24). Next, we examined FAM83A mRNA expression in primary epithelial cells generated from breast tissue biopsies of healthy women, and isogenic hTERT-immortalized and hTERT/RAS-transformed cells described in Kumar et al (25). FAM83A expression increased 6.2-fold in the immortalized cells (p=0.01), while only 4.3-fold in the transformed cells (p=0.03) (**Additional File 2**: **Supplementary Fig. 2B**). Both our findings and the data from Aran *et al* suggest that FAM83A is specifically activated in the early/intermediate phase of breast cancer development but has limited impact on the later phases of cancer progression.

FAM83A expression correlates with EGFR level

FAM83A protein has been reported as a possible key regulator in the EGFR pathway in breast cancer cells, leading to the development of resistance to tyrosine kinase inhibitors (TKIs) (6, 8). A recent report revealed a direct correlation between EGFR and FAM83A expression in NSCLC (12). We examined EGFR expression in both tumor and normal breast tissues and its correlation with FAM83A protein level (**Figure 3**). As previously reported (26), and in accordance with what observed in the METABRIC and TCGA cancer datasets (**Additional File 2**: **Supplementary Fig. 3**), EGFR expression is downregulated in tumors as compared with the normal breasts (2.4-fold change, p<0.0001 for positivity, 2.6-fold, p<0.0001 for H-score; **Figure 3A**). Nevertheless, EGFR expression in BC is directly correlated with FAM83A levels (r=0.28 for positivity and r=0.25 for H-score, both at p<0.0001) (**Figure 3B**).

A 1.2-fold overexpression of EGFR protein was also detected in tissues from women at high risk for BC as compared to the average-risk group (**Figure 3C** and **D**). However, the difference in EGFR expression between the two groups was significant only for the positivity analysis (p=0.01) and not for the H-score analysis (p=0.11). Pearson's correlation analysis revealed a direct correlation between the EGFR and FAM83A expression levels in normal breast tissues (r=0.40 for positivity and r=0.33 for H-score, both at p<0.0001) (**Figure 3E**). Data suggest that FAM83A may be involved in the EGFR signaling in both normal and cancer cells.

FAM83A overexpression promotes metabolic activation and cell proliferation of primary breast epithelial cells

To investigate the functional role of FAM83A in normal breasts as well as in cell transformation, we employed mGFP tagged-lentivirus infection to manipulate FAM83A expression in both primary and hTERT-immortalized epithelial cells (**Figure 4A, B** and **C**). Primary breast epithelial cells were isolated as previously described (15) from the cryopreserved breast tissue cores of average-risk women, and then infected with hTERT-expressing lentivirus. We next sought to determine whether FAM83A overexpression or loss impacted proliferation capacity or survival. First, cell viability and proliferation were monitored using *Sulforhodamine B* and bromodeoxyuridine (BrdU) incorporation assays, respectively (**Figure 4**). Compared with control cells, both cell viability (up to 90% at 48h and 3.4-fold at 72h, p>0.05) and proliferation rate (up to 47%, p<0.05) of FAM83A-overexpressing primary epithelial cells were significantly increased (**Figure 4D** and **E**). However, after downregulating the expression of FAM83A in primary epithelial cells, a reduction in cell viability was detected (22% and 31%, p=0.003 and p=0.04 respectively at 48hr; 25% and 26%. p=0.03 and p=0.04 respectively at 72h), whereas no change in cell proliferation was observed (**Figure 4D** and **E**). In the immortalized cells, the overexpression of FAM83A induced a significant increase in both cell viability and proliferation as compared with the control cells (p<0.05, **Figure 4F** and **G**). In contrast, when the expression of FAM83A was downregulated the cell viability and proliferation rate of immortalized breast epithelial cells significantly decreased compared with those of control cells (p<0.05; **Figure 4F** and **G**).

Next we assessed how FAM83A overexpression impacted the expression of survival- and proliferation-related genes in primary epithelial cells (**Figure 4H**). Because of the limited growth rate of the shFAM83A-primary cells and limited RNA yield, the transcriptome profiling generated a small number of reads (<15,000), below the appropriate threshold, and therefore the data were not included in any further analysis. FAM83A overexpression in primary epithelial cells induced the expression of Bcl2; however, no other apoptosis-related genes were affected. Cell proliferation genes such as MKI67, PCNA, BUB1 and the cell cycle regulator CCNB1 were also induced by FAM83A overexpression, thus reflecting the increase in cell viability and proliferation observed in these cells when compared with the control cells.

Transcriptome profiling of either FAM83A- or mock (control)-overexpressing primary cells was performed followed by differential expression analysis using DeSeq2 (**Additional File 1**: **Table S4**). Upon FAM83A overexpression in primary epithelial cells, 234 genes transcripts were downregulated, whereas 125 genes

were upregulated compared with the control (mock)-expressing cells (fold change:2, $p<0.05$). The majority of the genes affected by FAM83A overexpression were involved in cell adhesion ($p=0.0003$), epithelial mesenchymal transition ($p=0.0003$), metabolism ($p=0.005$) and estrogen biosynthesis ($p=0.0003$. The latter included downregulated genes only (**Figure 5A**). Molecular networks including the differentially expressed genes between FAM83A-overexpression and control and with a score >30 were the following: Cancer and endocrine system disorders (score 45), Cancer and cell morphology (score 38), and Carbohydrate metabolism (score 31) (**Figure 5B**).

FAM83A shows unique interaction partners in primary and immortalized epithelial cells.

To determine the mechanism of action of FAM83A in epithelial cells, protein interaction partners were also investigated. GFP-tagged FAM83A was overexpressed in either primary or hTERT-immortalized breast epithelial cells. Affinity purification with anti-GFP antibody combined with mass spectrometry (AP-MS) was used for protein–protein interactions mapping (27). Only targets associated with more than 20 peptides detected in the FAM83A overexpressing samples were considered for the analysis. Moreover, because a large number of nonspecific interactors, also contaminants, are co-purified with bait proteins and identified by MS, previously identified contaminants were selected and removed from the analysis (28, 29). In primary epithelial cells two proteins were found interacting with FAM83A: the helicase DDX3X and laminin subunit beta-3, LAMB3 (**Table 1** and Additional File 1: **Table S5**). While the first is involved in post-transcriptional regulation (30), LAMB3 plays a role in cell growth and cell adhesion (31). In the hTERT-immortalized cells FAM83A interacts with four molecules including LIMA1, PLEC, MYL6 and MYH10, involved in cytoskeleton reorganization.

Discussion

FAM83A is overexpressed in a variety of human tumors including lung, breast, testicular, and bladder cancers, suggesting that FAM83A may play a pro-oncogenic role in the development of cancer (2, 32, 33). Here, we investigated FAM83A association with breast cancer (BC) susceptibility by examining its expression in normal and BC tissues, and evaluating its functional role in the normal breast epithelial cells. Because the mechanism of FAM83A-promoting breast cancer is not clear, we explored both transcriptome alterations downstream FAM83A overexpression/downregulation, and FAM83A interaction partners in both primary and immortalized breast epithelial cells.

We recently reported the upregulation of FAM83A in the breast tissue from women at high risk of developing breast cancer (Tyrer-Cuzick lifetime risk score>20%), suggesting its potential role in breast cancer susceptibility (5). Notably, in this study we observed FAM83A upregulation not only in BC cases but also in breast tissue prior breast cancer diagnosis (pre-diagnosis or “susceptible”) compared to age-matched healthy controls. By using data from the GTEx and TCGA databases, Aran *et al* reported a transcriptome profiling of the normal breasts, tumor and histologically normal breast tissue adjacent to the tumor (NAT). The authors described the NAT as an intermediate state, representing not just a gradient

between tumor and healthy tissue, but a distinct tissue phenotype. They identified 82 genes that were upregulated in NAT compared with both healthy tissue and tumor. Among those FAM83A expression increased in the NAT compared with either the normal breast (logFoldChange: 3.96, p=9.9E-20) or the tumor tissue (logFoldChange: 2.69, p=1.0E-18) (24). Together the data suggest that FAM83A may have an important role in the early phase of breast cancer development than in late phase when the tumor mass is well-defined and oncogenic pathways prevail.

In regard to FAM83A expression in BC, previous transcriptomic and proteomic studies revealed that FAM83A is upregulated in HER2+ BCs, including those that are resistant to the HER2-targeted therapy trastuzumab (8, 34). HER2 is amplified in about 30% of all breast cancer patients and is a member of the same receptor tyrosine kinase family as EGFR, the ErbB family. In our immunohistochemical analysis, including 411 normal and 349 BC cases, we detected an equal expression of FAM83A among ER, PR, and HER2+ BC. FAM83A was not significantly overexpressed in triple negative BC as compared with normal breasts, and its protein expression increased mostly in the early BC stages (T1 and T2) rather than in later stages (T3 and T4). Nevertheless, as previously reported (13), Kaplan-Meier survival curves from the cancer cohort indicated that high FAM83A levels correlate with shortened survival time and poor prognosis in BC patients. Though initially this may seem to contradict our hypothesis that FAM83A is critical to the earliest phases of BC initiation, and less so to cancer local progression and invasion, we propose at least two explanations for FAM83A's resurgent expression in advanced disease: (1) FAM83A's involvement in treatment resistance (6); and (2), as observed in other tumor types (10), FAM83A's role in the late phase of breast tumorigenesis, potentially metastatic disease, which has not been investigated here. Our results provide strong evidence for a critical role of FAM83A in early phase of BC development, and, as such, it should be explored as a therapeutic target.

The ErbB family consists of four homologous RTKs: ErbB1/EGFR, ErbB2/HER2/Neu, ErbB3/HER3, and ErbB4/HER4. The ErbB signaling network tightly controls normal cell growth and proliferation through the activation of the RAS/MAPK and PI3K/AKT/mTOR pathways, Signal Transducer and Activator of Transcription 3 (STAT3), and Phospholipase D, among others. (35). Precision therapies aimed at disrupting ErbB RTKs (erlotinib, gefitinib, cetuximab, lapatinib, trastuzumab, pertuzumab), and downstream pathway (RAS-, RAF-, MEK-, PI3K/AKT/mTOR pathway inhibitors) are currently approved for patient use or are being evaluated in a number of clinical trials (36-39). Previous studies report that breast cancer cell lines with higher FAM83A expression (T47D, MCF7, MDA-MB361, MDA-MB468, and MDA-MB231) were more resistant to EGFR-TKI than cell lines with moderate expression (SKBR and T4-2) (6). In our analysis we found a direct correlation between FAM83A and EGFR protein levels stronger in normal (r=0.4, p<0.0001) than in BC (r=0.2, p<0.0001) samples suggesting that FAM83A may be involved in the EGFR-driven proliferative pathway in the normal breast and early phase of BC development rather than only in the advanced BC as previously described (6).

FAM83A was reported to drive HMEC transformation and confer resistance to EGFR-TKIs (6). Overexpressing FAM83A *in vitro* enhanced cell proliferation and invasiveness of a variety of cancer cell lines, including human lung (32, 40), pancreatic (11) and breast cancer (6). Depletion of FAM83A by

shRNA in malignant HMT3522 T4-2 HMECs and the breast cancer cell line MDA-MB-468 led to reduced invasiveness, proliferation rate, clonogenic potential, and tumor volume in immunocompromised mice (2, 6). However, FAM83A knockdown promoted tumor growth and invasion in human cervical cancer cell lines HeLa and CaSki (41). FAM83A depletion in breast cancer cells leads to suppressed proliferation and invasiveness in vitro as well as to suppressed tumor growth in vivo (2). In our study, FAM83A overexpression in primary epithelial cells induced both cell viability and proliferation. Furthermore, as previously reported (6), FAM83A overexpression in immortalized breast epithelial cells also promoted both cell viability and proliferation. However, while FAM83A downregulation in primary epithelial cells decreased the SRB staining (used to measure cell viability), probably reflecting a reduction in cell metabolism, no effect on BrdU incorporation (used to measure cell proliferation) was observed. This is the first study describing the effect of FAM83A overexpression in primary breast epithelial cells. Our data suggest that, FAM83A has pro-oncogenic role in early phase of BC development as shown in the immortalized cells, whereas in primary cells FAM83A affects cell growth but it is not a key regulator. The transcriptome analysis of FAM83A overexpressing primary cells confirmed the influence of FAM83A on cell metabolism and pro-oncogenic signaling pathways, including epithelial mesenchymal transition (ZEB1) and cell adhesion (ADAMs, (42)).

Finally, we further investigated FAM83A's mechanism of action in both primary and immortalized breast epithelial cells by searching for potential interaction partners. Among the eight FAM83 family genes (FAM83A-H), the 434-amino acid FAM83A protein is the smallest one. It contains DUF1669, serine-rich domains, and proline-rich domains (PRDs) (6). A conserved PxxP motif in the PRD domain interacts with Src homology 3 domain-containing proteins (43). A pseudo-PLD-like catalytic motif is contained in the DUF1669 domain, yet FAM83 proteins do not exhibit phospholipase activity. Recently it was found that the DUF1669 domain of FAM83 family proteins anchored casein kinase 1 isoforms which are implicated in the regulation of many cellular processes (7). Co-immunoprecipitation experiments revealed that FAM83A interacts with both c-Raf and the p85 regulatory subunit of PI3K (6). These endogenous interactions, as well as tyrosine phosphorylation of FAM83A, increase following stimulation with EGF. Taken together, these findings suggest that FAM83A can be phosphorylated upon EGFR activation, and that phosphorylation may be important for FAM83A-mediated signaling complex formation. Additional work will be needed to identify how FAM83A phosphorylation may regulate signaling complex formation and FAM83A-mediated transformation. Upon performing an affinity mass spectrometry experiment, we observed that in both primary and immortalized cells FAM83A binds actin filaments related protein and KEGG pathway investigation associates the identified targets with tight junction (MYHL6, MYH10) and focal adhesion/ECM- receptor interaction (LAMB3). Lee *et al.* reported that FAM83A depletion caused actin stress fibers to become primarily cortical leading to reduced invasiveness (6). Notably, another FAM83A interaction partner in primary cells is DDX3X, a molecule of interest in cancer biology for its involvement in cell cycle, apoptosis and cell migration through regulation of transcription, mRNA maturation, mRNA export and translation (30).

Although this is the first report using a large cohort of either normal or cancerous breast tissues to investigate FAM83A's protein expression, and analyzing FAM83A's functional role in primary breast

epithelial cells, the study bears several limitations. Because 92% of the tumor cohort consisted of ductal/lobular invasive disease, our analysis lacked of the FAM83A staining data on the earlier premalignant lesions. While we tried to address this point by analyzing the susceptible normal breast cohort (Fig.2), the analysis of early phase of BC in the PreCancer Atlas may provide better clues on the significance on FAM83A in BC progression (44). Furthermore, while new interaction partners for FAM83A in both primary and immortalized cells were identified, the functional impact of such interaction requires further investigation. Previous studies demonstrated that the elevated FAM83A expression observed in numerous tumor types could be due to genomic amplification of 8q24, which also contains the oncogene Myc (11). It would be interesting to evaluate the correlation between FAM83A level and 8q24 amplification in our cohort, and examine other potential mechanisms responsible for FAM83A induction.

Conclusion

In summary, our study elucidates the critical role of FAM83A in breast cancer initiation. When compared with its level in normal breast, FAM83A shows an increased expression in both breast tumors and, to a greater extent, in early phase of BC development, as suggested by our data on susceptible normal breast and Aran *etal*'s data on NAT (24). Moreover, FAM83A overexpression in primary cells induced metabolic activation and cell proliferation, two hallmarks of cancer initiation. Our study also demonstrates the importance of examining the normal breast tissue to decipher the molecular aberrations occurring in early breast cancer development. Understanding the earliest changes in malignant transformation will be critical to eventually preventing this disease altogether.

Abbreviations

BC: breast cancer; **KTB:** Susan G. Komen Tissue bank at IU Simon Comprehensive Cancer Center; **TMA**: Tissue MicroArray; **IPA**: Ingenuity pathway analysis; **Susc**: susceptible; **HC**: Healthy Control.

Declarations

Ethics approval and consent to participate: Normal breast and breast cancer (BC) TMAs were obtained from the Susan G. Komen Tissue Bank at IU Simon Comprehensive Cancer Center (KTB) under Institutional Review Board (IRB) protocol #1011003097 and IUSCCC Tissue Procurement and Distribution Core under IRB protocol #**11438**, respectively. Specimens were collected upon informed consent of either healthy volunteer women (KTB) or breast cancer cases.

Consent for publication: Not applicable

Availability of data and materials: The dataset including transcriptome profiling of microdissected breast epithelium form either susceptible normal breast biopsies or healthy controls was retrieved from the Gene Expression Omnibus (GEO) repository, access number GSE141828 (https://www.ncbi.nlm.nih.gov/geo/query/acc.cgi?acc=GSE141828). The dataset including

transcriptome profiling of susceptible breast samples and age-matched healthy control is available in GEO (accession number GSE166044, https://www.ncbi.nlm.nih.gov/geo/query/acc.cgi?acc=GSE166044). The transcriptome data (raw counts) for the FAM83A- or CTR-overexpressing primary cells are included in Additional File 1: Table S4. The mass spectrometry data (raw counts) for the FAM83A- or CTR-overexpressing primary and hTERT immortalized cells are included in Additional File 1: Table S5.

Competing interests: The authors have no conflicts of interest to disclose.

Funding: The work including sample processing, data collection and analysis was funded by the Breast Cancer Research Foundation (BCRF-19-155 and BCRF-20-155 to A.M.S) and the Hero Foundation. The Susan G. Komen Tissue Bank at the IU Simon Comprehensive Cancer Center (IUSCCC) is supported by the IUSCCC, Susan G. Komen, and the Vera Bradley Foundation for Breast Cancer Research.

Authors' contributions: N.M. conceived the idea and designed the experiments, analyzed, and interpreted the data, and was major contributor in writing the manuscript. N.M. and RG performed the experiments and generated the data. R.P. performed the bioinformatics analysis. S.A. performed the statistical analysis. C.T. performed the immunostaining of the tissue microarray. G. S., R.J. and B.S. analyzed the Tissue Microarray staining data. P.R. provided the specimens used in this study. H.N. provided input on the project. A.M.S. funded the work and contributed to the manuscript preparation. All the authors read and approved the manuscript.

Acknowledgements: We thank the women who donated their tissue specimens to either the Tissue Procurement & Distribution Core (Grant P30 CA082709) or the Susan G. Komen Tissue Bank both at IU Simon Comprehensive Cancer Center (IUSCCC). We thank the Pathology Lab for the immunostaining and analysis of the tissue microarrays, the Proteomic Core for the mass spectrometry analysis, and the Center for Medical Genomics for the RNA sequencing analysis.

References

1. Snijders AM, Lee SY, Hang B, Hao W, Bissell MJ, Mao JH. FAM83 family oncogenes are broadly involved in human cancers: an integrative multi-omics approach. Mol Oncol. 2017;11(2):167-79.
2. Cipriano R, Miskimen KL, Bryson BL, Foy CR, Bartel CA, Jackson MW. Conserved oncogenic behavior of the FAM83 family regulates MAPK signaling in human cancer. Mol Cancer Res. 2014;12(8):1156-65.
3. Bartel CA, Parameswaran N, Cipriano R, Jackson MW. FAM83 proteins: Fostering new interactions to drive oncogenic signaling and therapeutic resistance. Oncotarget. 2016;7(32):52597-612.
4. Cipriano R, Graham J, Miskimen KL, Bryson BL, Bruntz RC, Scott SA, et al. FAM83B mediates EGFR- and RAS-driven oncogenic transformation. J Clin Invest. 2012;122(9):3197-210.
5. Marino N, German R, Podicheti R, Rush DB, Rockey P, Huang J, et al. Aberrant epigenetic and transcriptional events associated with breast cancer risk. bioRxiv. 2021.

6. Lee SY, Meier R, Furuta S, Lenburg ME, Kenny PA, Xu R, et al. FAM83A confers EGFR-TKI resistance in breast cancer cells and in mice. J Clin Invest. 2012;122(9):3211-20.
7. Fulcher LJ, Bozatzi P, Tachie-Menson T, Wu KZL, Cummins TD, Bufton JC, et al. The DUF1669 domain of FAM83 family proteins anchor casein kinase 1 isoforms. Sci Signal. 2018;11(531).
8. Bartel CA, Jackson MW. HER2-positive breast cancer cells expressing elevated FAM83A are sensitive to FAM83A loss. PLoS One. 2017;12(5):e0176778.
9. Grant S. FAM83A and FAM83B: candidate oncogenes and TKI resistance mediators. J Clin Invest. 2012;122(9):3048-51.
10. Zhou F, Geng J, Xu S, Meng Q, Chen K, Liu F, et al. FAM83A signaling induces epithelial-mesenchymal transition by the PI3K/AKT/Snail pathway in NSCLC. Aging (Albany NY). 2019;11(16):6069-88.
11. Chen S, Huang J, Liu Z, Liang Q, Zhang N, Jin Y. FAM83A is amplified and promotes cancer stem cell-like traits and chemoresistance in pancreatic cancer. Oncogenesis. 2017;6(3):e300.
12. Richtmann S, Wilkens D, Warth A, Lasitschka F, Winter H, Christopoulos P, et al. FAM83A and FAM83B as Prognostic Biomarkers and Potential New Therapeutic Targets in NSCLC. Cancers (Basel). 2019;11(5).
13. Pawitan Y, Bjohle J, Amler L, Borg AL, Egyhazi S, Hall P, et al. Gene expression profiling spares early breast cancer patients from adjuvant therapy: derived and validated in two population-based cohorts. Breast Cancer Res. 2005;7(6):R953-64.
14. Sandusky GE, Mintze KS, Pratt SE, Dantzig AH. Expression of multidrug resistance-associated protein 2 (MRP2) in normal human tissues and carcinomas using tissue microarrays. Histopathology. 2002;41(1):65-74.
15. Marino N, German R, Rao X, Simpson E, Liu S, Wan J, et al. Upregulation of lipid metabolism genes in the breast prior to cancer diagnosis. NPJ Breast Cancer. 2020;6:50.
16. Prasad M, Kumar B, Bhat-Nakshatri P, Anjanappa M, Sandusky G, Miller KD, et al. Dual TGFbeta/BMP Pathway Inhibition Enables Expansion and Characterization of Multiple Epithelial Cell Types of the Normal and Cancerous Breast. Mol Cancer Res. 2019;17(7):1556-70.
17. Burriss KH, Mosley AL. Methods review: Mass spectrometry analysis of RNAPII complexes. Methods. 2019;159-160:105-14.
18. Dobin A, Davis CA, Schlesinger F, Drenkow J, Zaleski C, Jha S, et al. STAR: ultrafast universal RNA-seq aligner. Bioinformatics. 2013;29(1):15-21.
19. Kramer A, Green J, Pollard J, Jr., Tugendreich S. Causal analysis approaches in Ingenuity Pathway Analysis. Bioinformatics. 2014;30(4):523-30.
20. Curtis C, Shah SP, Chin SF, Turashvili G, Rueda OM, Dunning MJ, et al. The genomic and transcriptomic architecture of 2,000 breast tumours reveals novel subgroups. Nature. 2012;486(7403):346-52.
21. Pereira B, Chin SF, Rueda OM, Vollan HK, Provenzano E, Bardwell HA, et al. The somatic mutation profiles of 2,433 breast cancers refines their genomic and transcriptomic landscapes. Nat Commun.

2016;7:11479.

22. Chandrashekar DS, Bashel B, Balasubramanya SAH, Creighton CJ, Ponce-Rodriguez I, Chakravarthi B, et al. UALCAN: A Portal for Facilitating Tumor Subgroup Gene Expression and Survival Analyses. Neoplasia. 2017;19(8):649-58.
23. Fletcher O, Johnson N, Gibson L, Coupland B, Fraser A, Leonard A, et al. Association of genetic variants at 8q24 with breast cancer risk. Cancer Epidemiol Biomarkers Prev. 2008;17(3):702-5.
24. Aran D, Camarda R, Odegaard J, Paik H, Oskotsky B, Krings G, et al. Comprehensive analysis of normal adjacent to tumor transcriptomes. Nat Commun. 2017;8(1):1077.
25. Kumar B, Prasad M, Bhat-Nakshatri P, Anjanappa M, Kalra M, Marino N, et al. Normal Breast-Derived Epithelial Cells with Luminal and Intrinsic Subtype-Enriched Gene Expression Document Interindividual Differences in Their Differentiation Cascade. Cancer Res. 2018;78(17):5107-23.
26. Flageng MH, Knappskog S, Haynes BP, Lonning PE, Mellgren G. Inverse regulation of EGFR/HER1 and HER2-4 in normal and malignant human breast tissue. PLoS One. 2013;8(8):e74618.
27. Gingras AC, Gstaiger M, Raught B, Aebersold R. Analysis of protein complexes using mass spectrometry. Nat Rev Mol Cell Biol. 2007;8(8):645-54.
28. Mellacheruvu D, Wright Z, Couzens AL, Lambert JP, St-Denis NA, Li T, et al. The CRAPome: a contaminant repository for affinity purification-mass spectrometry data. Nat Methods. 2013;10(8):730-6.
29. Hodge K, Have ST, Hutton L, Lamond AI. Cleaning up the masses: exclusion lists to reduce contamination with HPLC-MS/MS. J Proteomics. 2013;88:92-103.
30. Mo J, Liang H, Su C, Li P, Chen J, Zhang B. DDX3X: structure, physiologic functions and cancer. Mol Cancer. 2021;20(1):38.
31. Zhang H, Pan YZ, Cheung M, Cao M, Yu C, Chen L, et al. LAMB3 mediates apoptotic, proliferative, invasive, and metastatic behaviors in pancreatic cancer by regulating the PI3K/Akt signaling pathway. Cell Death Dis. 2019;10(3):230.
32. Hu H, Wang F, Wang M, Liu Y, Wu H, Chen X, et al. FAM83A is amplified and promotes tumorigenicity in non-small cell lung cancer via ERK and PI3K/Akt/mTOR pathways. Int J Med Sci. 2020;17(6):807-14.
33. Parameswaran N, Bartel CA, Hernandez-Sanchez W, Miskimen KL, Smigiel JM, Khalil AM, et al. A FAM83A Positive Feed-back Loop Drives Survival and Tumorigenicity of Pancreatic Ductal Adenocarcinomas. Sci Rep. 2019;9(1):13396.
34. Boyer AP, Collier TS, Vidavsky I, Bose R. Quantitative proteomics with siRNA screening identifies novel mechanisms of trastuzumab resistance in HER2 amplified breast cancers. Mol Cell Proteomics. 2013;12(1):180-93.
35. Avraham R, Yarden Y. Feedback regulation of EGFR signalling: decision making by early and delayed loops. Nat Rev Mol Cell Biol. 2011;12(2):104-17.

36. Ostrem JM, Peters U, Sos ML, Wells JA, Shokat KM. K-Ras(G12C) inhibitors allosterically control GTP affinity and effector interactions. Nature. 2013;503(7477):548-51.
37. Girotti MR, Lopes F, Preece N, Niculescu-Duvaz D, Zambon A, Davies L, et al. Paradox-breaking RAF inhibitors that also target SRC are effective in drug-resistant BRAF mutant melanoma. Cancer Cell. 2015;27(1):85-96.
38. Zhao Y, Adjei AA. The clinical development of MEK inhibitors. Nat Rev Clin Oncol. 2014;11(7):385-400.
39. Dienstmann R, Rodon J, Serra V, Tabernero J. Picking the point of inhibition: a comparative review of PI3K/AKT/mTOR pathway inhibitors. Mol Cancer Ther. 2014;13(5):1021-31.
40. Zheng YW, Li ZH, Lei L, Liu CC, Wang Z, Fei LR, et al. FAM83A Promotes Lung Cancer Progression by Regulating the Wnt and Hippo Signaling Pathways and Indicates Poor Prognosis. Front Oncol. 2020;10:180.
41. Xu J, Lu W. FAM83A exerts tumorsuppressive roles in cervical cancer by regulating integrins. Int J Oncol. 2020;57(2):509-21.
42. Przemyslaw L, Boguslaw HA, Elzbieta S, Malgorzata SM. ADAM and ADAMTS family proteins and their role in the colorectal cancer etiopathogenesis. BMB Rep. 2013;46(3):139-50.
43. Ferraro E, Peluso D, Via A, Ausiello G, Helmer-Citterich M. SH3-Hunter: discovery of SH3 domain interaction sites in proteins. Nucleic Acids Res. 2007;35(Web Server issue):W451-4.
44. Srivastava S, Ghosh S, Kagan J, Mazurchuk R. The PreCancer Atlas (PCA). Trends Cancer. 2018;4(8):513-4.

Figures

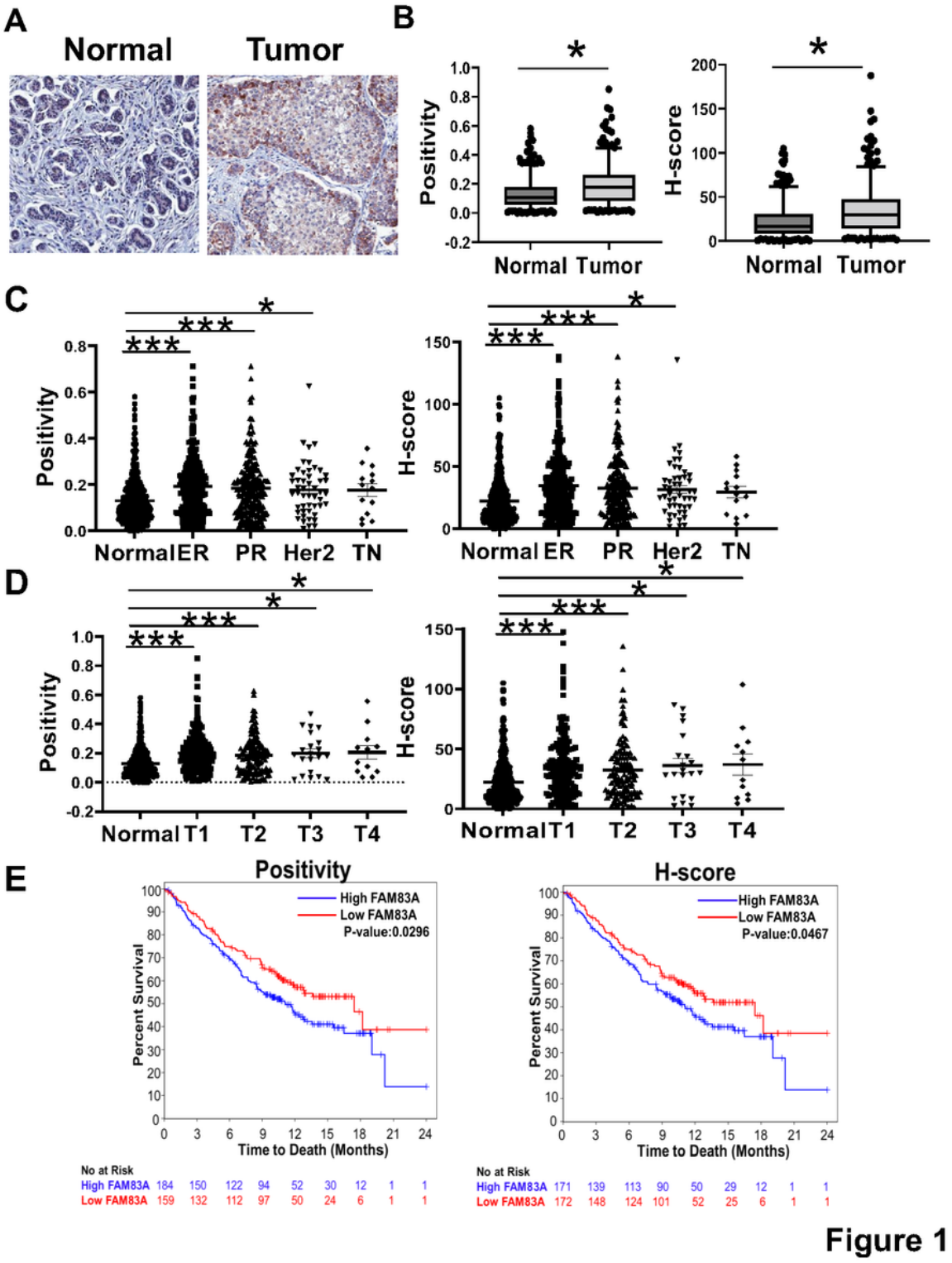

Figure 1

Figure 1

FAM83A expression in breast tumors. A) Representative images at 20 X magnification and (B) quantification of FAM83A staining of either normal or tumor breast tissue sections. Data are shown as box and whisker at 5th-95th percentile. C) FAM83A staining quantification in different breast cancer hormone receptor-based subtypes or (D) tumor stage (T1-T4) as compared with normal breast. Each dot represents a single subject data point. Data are shown as average ± standard error of the mean. E)

Kaplan–Meier survival curves of breast cancer patients based on FAM83A expression status for both positivity and H-score analyses (blue lines indicate patients with high FAM83A level; red lines indicate patients with low FAM83A level). ER: estrogen receptor, PR: progesterone receptor, Her2: HER2 gene amplification, TN: triple negative. *p<0.05.**p<0.001, ***p<0.0001.

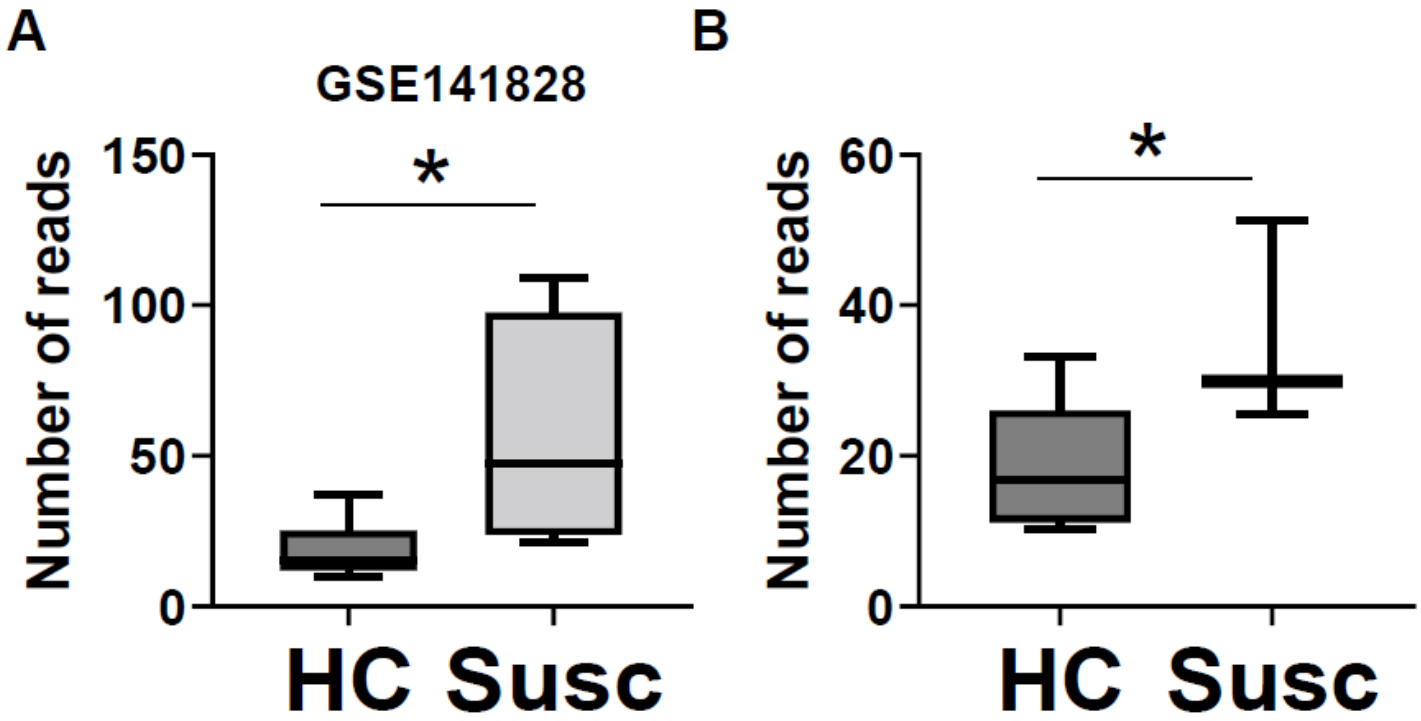

Figure 2

FAM83A expression in breast prior to cancer diagnosis. A) FAM83A expression in microdissected-epithelial breast tissues from either women prior their breast cancer diagnosis (Susc) or healthy women (healthy controls, HC). Data were retrieved from GEO, GSE141828. B) FAM83A expression in breast tissues from either women prior their breast cancer diagnosis (Susc) or healthy women (HC). *p<0.05.

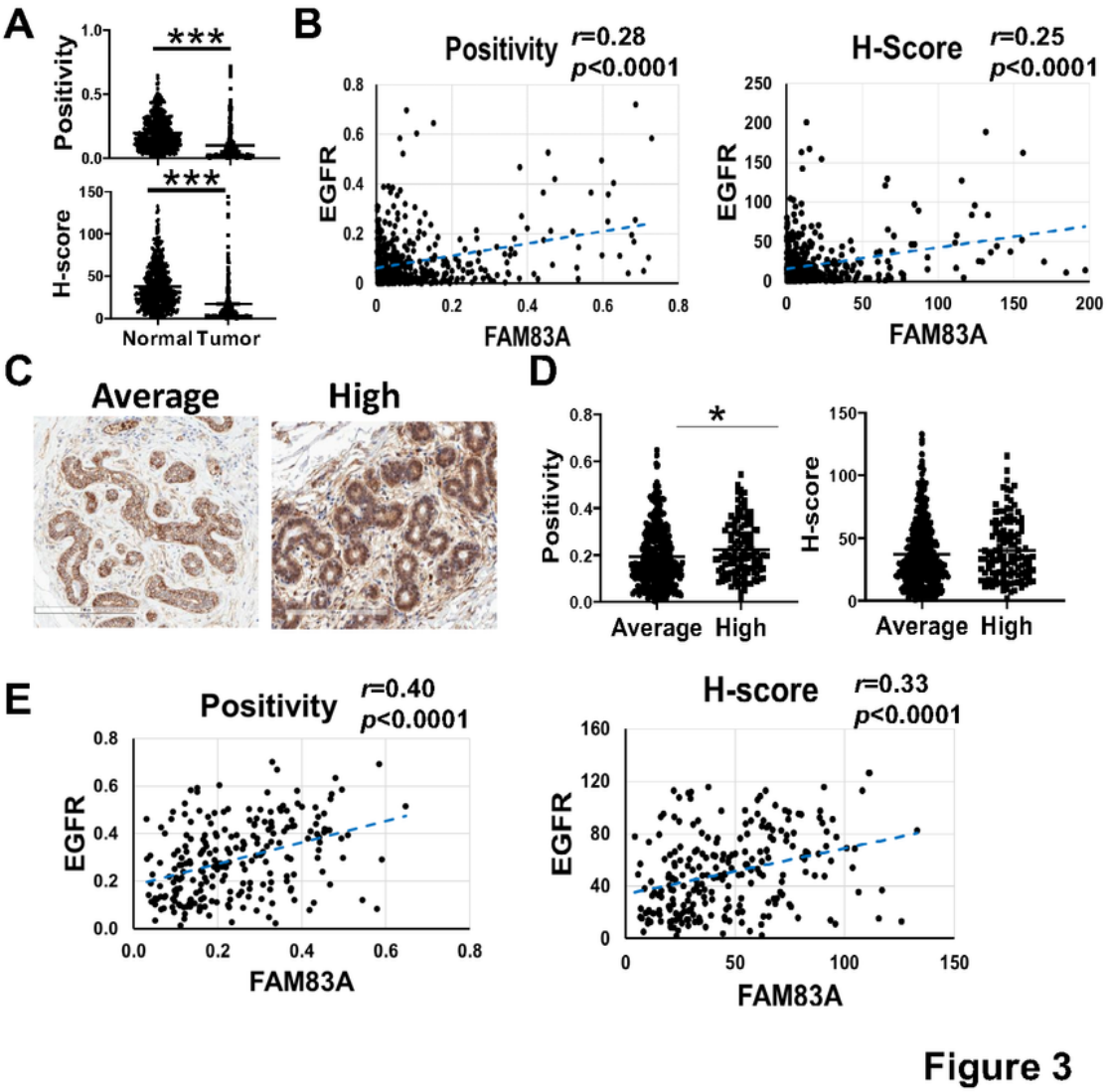

Figure 3

Figure 3

EGFR and FAM83A correlation in cancerous and normal breast. A) EGFR staining quantification in normal breast (N) and Tumor (T) tissues. Staining quantification of the two markers is expressed as positivity and H-score. Data are shown as mean ± standard error of the mean. B) Pearson's correlation between FAM83A and EGFR level in breast tumors. C) Representative images of EGFR staining of normal breast tissues from women at either average or high risk for breast cancer. 20X magnification is shown. D)

Quantification of EGFR staining of normal breast expressed as positivity and H-score. E) Pearson's correlation between FAM83A and EGFR level in normal breast tissues. *p<0.05, ***p<0.0001.

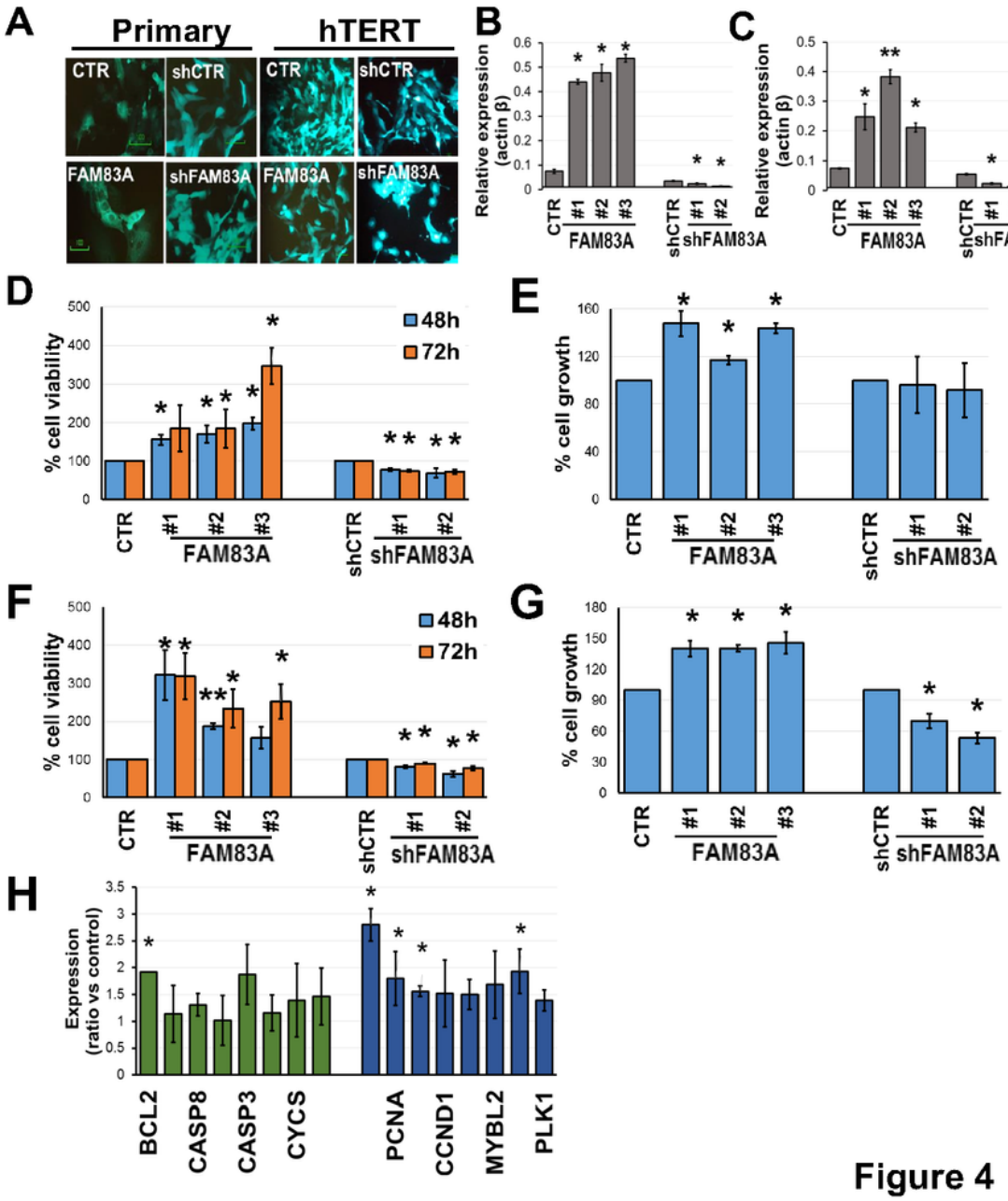

Figure 4

Figure 4

FAM83A overexpression promotes cell proliferation. A) Representative images of either mGFP-positive primary epithelial cells (N=3) or paired hTERT-immortalized cells after lentiviral infection to express either control mock (CTR), FAM83A (FAM83A), pLKO control (shCTR), or shRNA for FAM83A (shFAM83A). 20x

magnification images are shown and mGFP is in green. FAM83A expression in either primary (B) or immortalized (C) cells infected with either control, FAM83A-overexpression, or shFAM83A lentivirus particles. Cell viability and cell proliferation of primary (D and E) or immortalized (F and G) cells measured with SRB assay or BrdU assay, respectively. Data are shown as percentage of either cell viability or cell growth of the FAM83A overexpressing/downregulating cells versus the control cells. H) Expression of apoptosis (green bars) and cell proliferation (blue bars) related genes in primary epithelial cells either overexpressing or downregulating FAM83A. *p<0.05, **p<0.001.

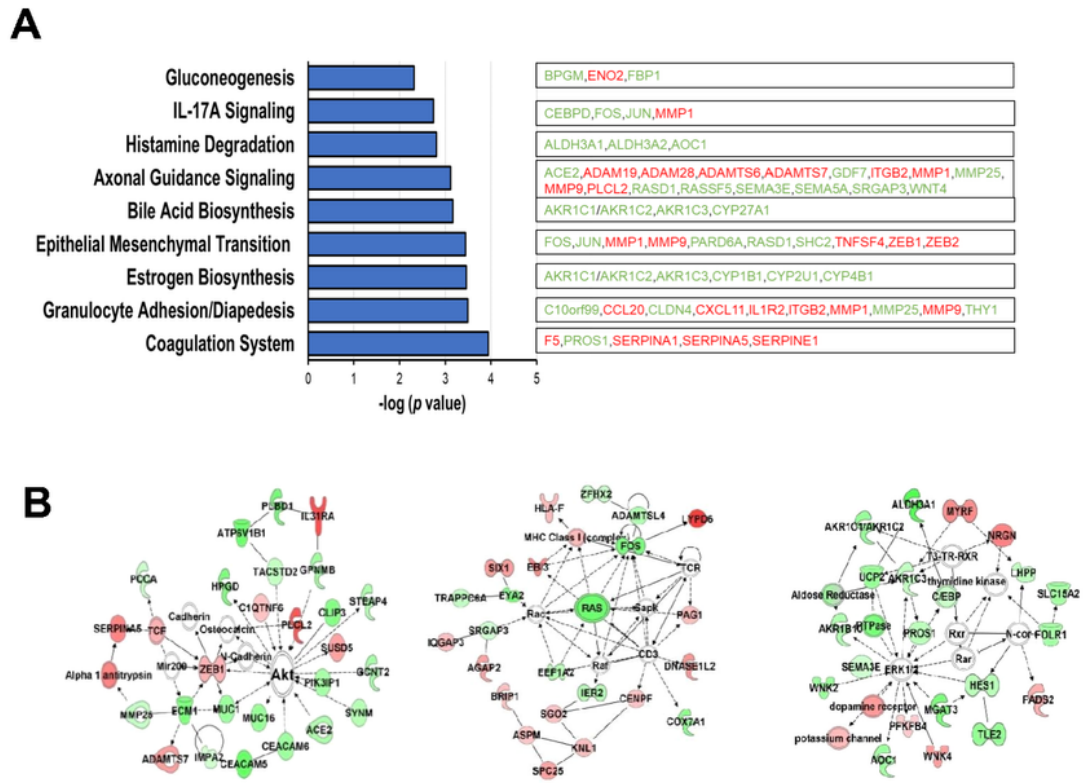

Figure 5

Figure 5

FAM83A overexpression induced metabolic pathway activation in primary epithelial cells. A) Ingenuity pathway analysis (IPA) revealed the canonical pathways linked with the genes differentially expressed between FAM83A-overexpressing and control cells. Downregulated genes are in green and upregulated genes are in red. B) Molecular networks linking the differentially expressed genes were obtained using IPA. Upregulated genes are shown in red while downregulated genes are in green and connecting molecules are white. The three networks shown in the figure include: 1. Cancer and endocrine system disorders; 2. Cancer and cell morphology; and 3. Carbohydrate metabolism.

Supplementary Files

This is a list of supplementary files associated with this preprint. Click to download.

- AdditionalFile1TablesS1S5.xlsx
- AdditionalFile2SupplementaryFig13.pdf